Scattering of 65-MeV Alpha Particles from ^{89}Y, ^{92}Zr, ^{94}Zr, ^{96}Zr, and ^{116}Sn†

C. R. BINGHAM

The University of Tennessee, Knoxville, Tennessee, and Oak Ridge National Laboratory, Oak Ridge, Tennessee 37830

AND

M. L. HALBERT AND A. R. QUINTON*

Oak Ridge National Laboratory, Oak Ridge, Tennessee 37830

(Received 2 December 1968)

Differential cross sections for the scattering of 65-MeV α particles from ^{89}Y, ^{94}Zr, ^{96}Zr, and ^{116}Sn were measured at 1° intervals between 10° and ~75°. Angular distributions previously reported for ^{92}Zr were extended to 112°. Several Woods-Saxon potentials were found to fit each elastic angular distribution. Distorted-wave calculations for the inelastic scattering were made with collective-model form factors. The deformation lengths βR_0 are generally in agreement with the results of other experiments. Calculations using shell-model form factors were made for the 2^+ and 4^+ states in ^{94}Zr; a somewhat better fit to the data was obtained than with the collective model.

I. INTRODUCTION

ANGULAR distributions were measured from 10° to ~70° lab for elastic scattering of 65-MeV α particles from ^{89}Y, ^{94}Zr, ^{96}Zr, and ^{116}Sn, and inelastic scattering from ^{94}Zr, ^{96}Zr, and ^{116}Sn. Inelastic spectra for ^{89}Y were obtained between 34° and 37°. This work represents a continuation of earlier measurements[1] on ^{90}Zr, ^{91}Zr, and ^{92}Zr. The data were analyzed in terms of a nonspherical optical model: The spherical part, a Woods-Saxon potential, gives the elastic scattering, and the nonspherical part, parametrized by the deformation parameter β, produces inelastic transitions.

As before,[1] when least-squares fits of the elastic data to angles below 80° were made, a smooth variation of the optical-model parameters over a very large range gave good fits. Beyond 80°, the angular distributions predicted by the different potentials were not the same. In an effort to remove the ambiguity, the ^{92}Zr(α, α) data of Ref. 1 were extended to 112° lab. At the same time, additional data on the two strongest inelastic transitions were obtained.

II. EXPERIMENTAL DETAILS

The measurements were performed in the 30-in.-diam scattering chamber at the Oak Ridge Isochronous Cyclotron with the slit and detector arrangement described previously.[1] The angular acceptance of the counters was about 1°. A (ΔE, E) counter telescope consisting of two silicon detectors was used to distinguish α and ^{3}He particles; the (α, ^{3}He) results will be published separately. No ΔE counter was used for the new data on ^{92}Zr, since the pulse heights of the elastic and the two strongest inelastic groups were well above the ^{3}He groups. These data were taken at two angles simultaneously with two silicon detectors. The cross sections from 43° to 56° (lab) were remeasured to determine the angle scale and to check the absolute normalization.

The targets were metal foils prepared by the ORNL Isotopes Development Center. The energy loss of ^{241}Am α particles in each target was measured and the target thicknesses were estimated to an accuracy of about ±10% by interpolation in the tables given by Whaling.[2] This uncertainty in target thickness is the main source of error in the measured cross sections. The thicknesses were between 5 and 8.5 mg/cm^2, except for a 1.2-mg/cm^2 ^{116}Sn target that was used for angles less than 50° and a 2-mg/cm^2 ^{89}Y target used to study inelastic peaks between 34° and 37°.

The over-all resolution for the ^{92}Zr, ^{94}Zr, ^{96}Zr, and most of the ^{89}Y spectra was 200–250 keV. For these targets, energy straggling in the targets was calculated to be 105 keV, the kinematic spread was no more than 80 keV, and the spread in beam energy was ~125 keV. The remainder of the spread was presumably due to the detectors. For the ^{116}Sn data, the beam energy spread was held to 65 keV. The resulting over-all resolution was ~110 keV for the thin target and ~140 keV for the thick target. For the ^{89}Y inelastic data the beam resolution was 125 keV and the total resolution was 180–200 keV.

A typical thin-target spectrum for ^{116}Sn is shown in Fig. 1. The ^{89}Y spectrum at 34.3° is shown in Fig. 2. The Zr spectra are similar to those of Ref. 1.

III. ELASTIC SCATTERING

The elastic scattering angular distributions are shown in Figs. 3–5 in comparison with optical-model least-squares fits. The potential used was of the Woods-Saxon form

$$V(r) = -[V_0/(1+e^x)] - [iW_0/(1+e^{x'})] + V_c,$$

† Research sponsored by the U.S. Atomic Energy Commission under contract with Union Carbide Corporation.

* Summer Research Participant from the University of Florida under appointment from Oak Ridge Associated Universities (1965); present address: University of Massachusetts, Amherst, Mass.

[1] C. R. Bingham, M. L. Halbert, and R. H. Bassel, Phys. Rev. **148**, 1174 (1966).

[2] W. Whaling, in *Handbuch der Physik*, edited by S. Flügge (Springer-Verlag, Berlin, 1958), Vol. 34, pp. 193–217.

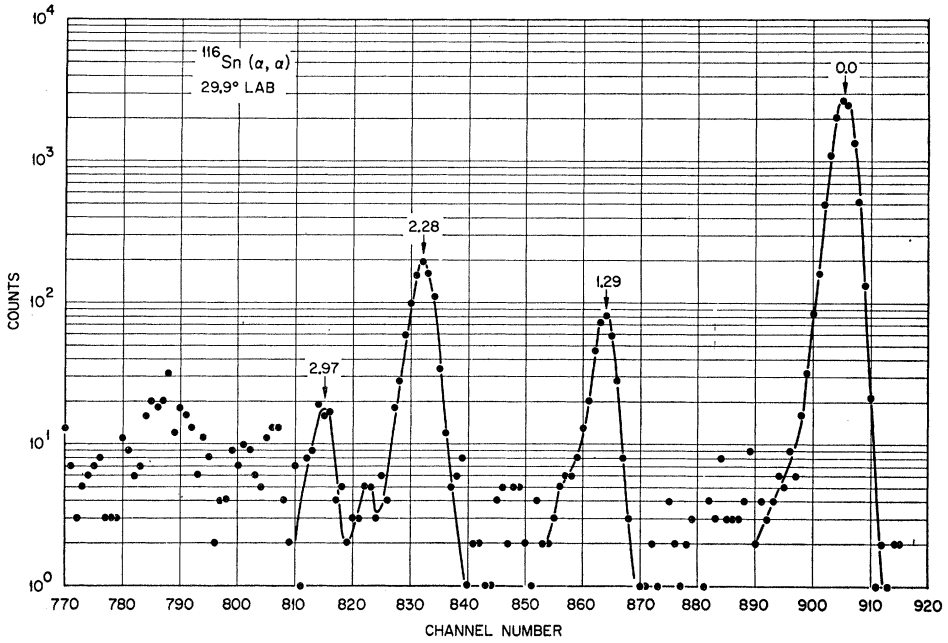

FIG. 1. α-particle spectrum at 29.9° lab from ^{116}Sn bombarded with 65.7-MeV α particles. The excitation energies of the inelastic peaks are given.

where $x=(r-r_0A^{1/3})/a$, $x'=(r-r_0'A^{1/3})/a'$, and V_c is the Coulomb potential for a uniformly charged sphere of radius 1.4 $A^{1/3}$ F. The free parameters V_0, r_0, a, W_0, r_0', and a' were adjusted with an automatic search routine[3] to minimize the quantity

$$\chi^2=\sum_i[(\sigma_{\rm th}^{(i)}-\sigma_{\rm expt}^{(i)})/\Delta\sigma_{\rm expt}^{(i)}]^2,$$

where $\sigma_{\rm th}^{(i)}$ and $\sigma_{\rm expt}^{(i)}$ are the calculated and experimental cross sections at angle θ_i, and $\Delta\sigma_{\rm expt}^{(i)}$, the weighting factor, is related to the estimated accuracy of $\sigma_{\rm expt}^{(i)}$. For the searches described here, the $\sigma_{\rm expt}^{(i)}$ were chosen to be 5–10% of $\sigma_{\rm expt}^{(i)}$ for most of the points. For ^{89}Y and the Zr isotopes, values up to 50% of $\sigma_{\rm expt}^{(i)}$ were used for a few points near the minima where the cross section is changing rapidly over the

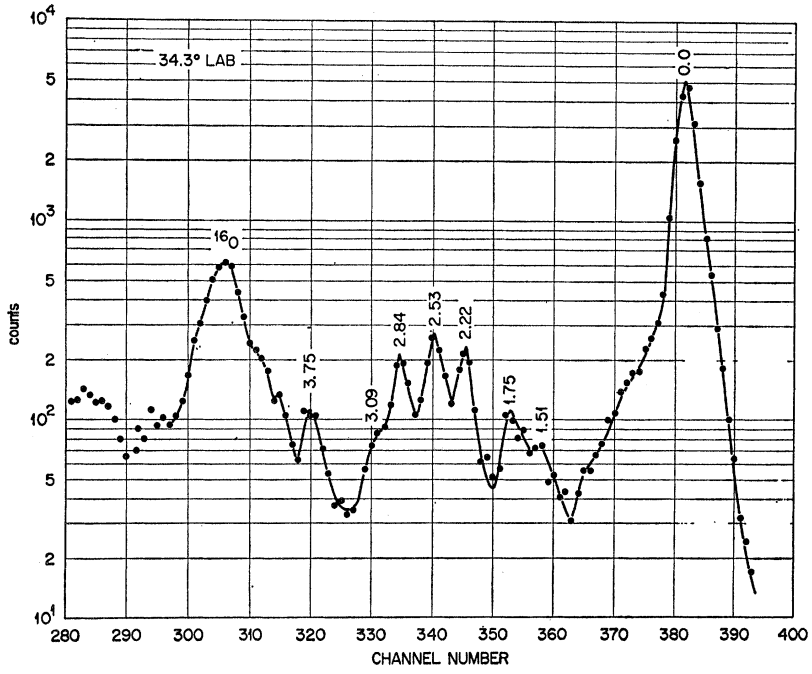

FIG. 2. α-particle spectrum at 34.3° lab from ^{89}Y bombarded with 65.0-MeV α particles. The excitation energies of the excited peaks are given.

[3] R. M. Drisko, HUNTER program (unpublished).

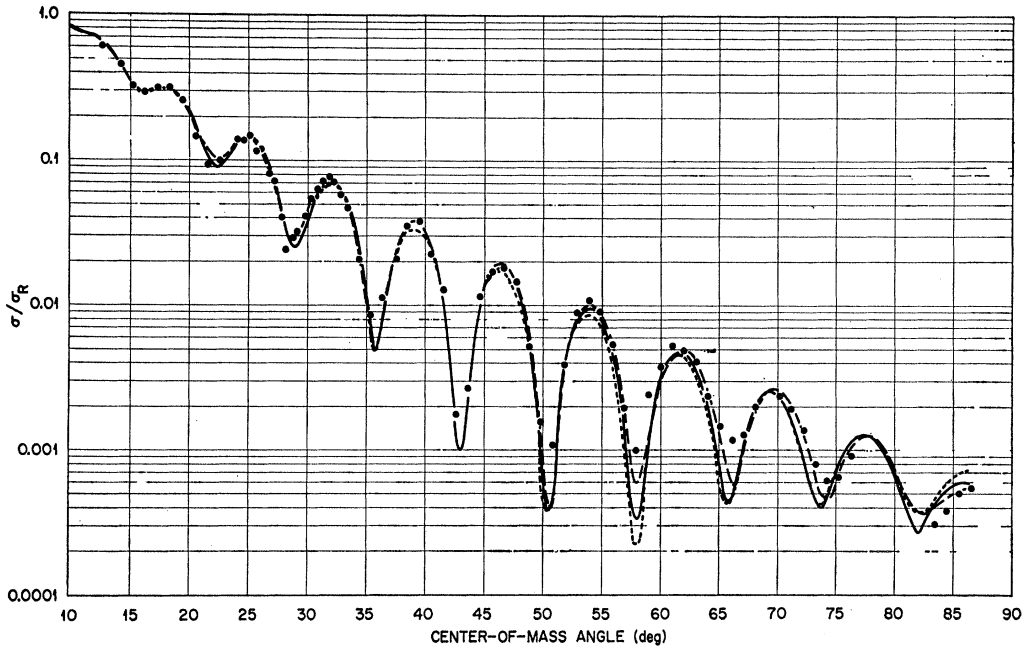

FIG. 3. Ratio of the elastic scattering cross section to the Rutherford cross section for 65.7-MeV α particles on ^{116}Sn. The smooth curves are optical-model least-squares fits obtained with potentials: *A* (solid line), *B* (long-dashed line), and *C* (short-dashed line).

aperture of the detector. For most of the searches involving data to ~75°, the restriction $x=x'$ was made, so that only four free parameters were used.

Three different fits to the ^{116}Sn(α, α) angular distribution are shown in Fig. 3. The corresponding optical-model parameters, values of the predicted reaction cross section σ_r, and values of χ^2 are given in Table I. As before,[1] among the four-parameter fits there was a slight preference for $V_0 \approx 35$ MeV. A slight reduction in χ^2 was obtained by allowing six parameters to vary (potential *B*). Both of the shallow potentials (*A* and *B*) correspond to discrete minima in χ^2. Potentials *C* and *D*, however, are only two representative points of a continuous ambiguity in the potential (see Ref. 1). The fits of the angular distribution with all of these potentials are very similar, and Fig. 3 shows only the fit with potential *C*. Also shown in Table I are the best-fit potentials for ^{89}Y, ^{94}Zr, and ^{96}Zr near $V_0=35$ MeV. A continuous ambiguity exists for these nuclei also and one representative point is shown for each nucleus. The corresponding fits of the data are shown in Fig. 4.

Figure 6 shows the interdependence of the optical-model parameters for ^{116}Sn, ^{89}Y, ^{58}Ni, and the five Zr

TABLE I. Optical-model potentials from elastic scattering of α particles.

Target	Potential	E_a (MeV)	V_0 (MeV)	W_0 (MeV)	r_0 (F)	a (F)	σ_r (mb)	χ^2
^{116}Sn	*A*	65.7	36.9	21.7	1.505	0.648	2098	612
^{116}Sn	*B*[a]	65.7	41.68	13.21	1.467	0.669	2185	448
^{116}Sn	*C*	65.7	100.0	53.7	1.352	0.667	2082	749
^{116}Sn	*D*	65.7	200.0	102.9	1.254	0.669	2077	724
^{89}Y	*E*	65.0	34.6	17.71	1.557	0.648	1963	117
^{89}Y	*F*	65.0	125.0	54.78	1.365	0.635	1922	240
^{94}Zr	*G*	65.0	35.4	20.7	1.545	0.656	2041	235
^{94}Zr	*H*	65.0	125.0	66.2	1.346	0.661	2014	347
^{96}Zr	*I*	65.0	37.0	22.1	1.534	0.656	2063	297
^{96}Zr	*J*	65.0	125.0	67.6	1.346	0.660	2040	364

[a] Six-parameter potential with $r_0'=1.589$, $a'=0.713$.

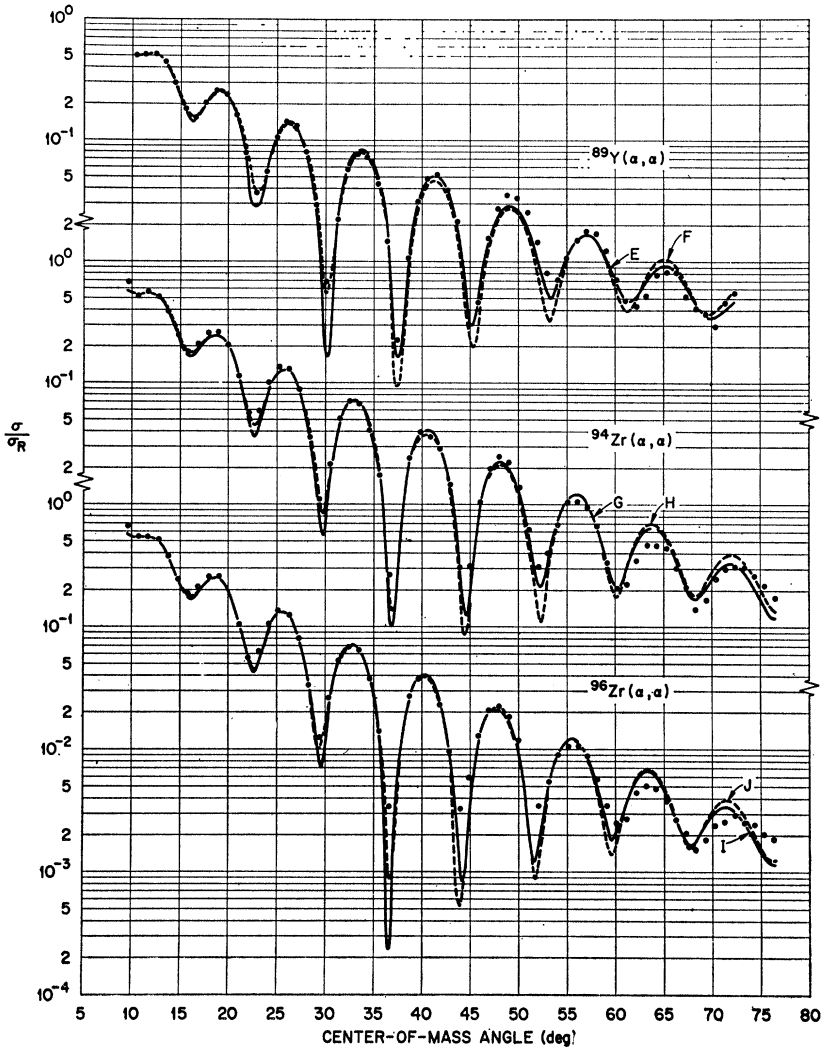

FIG. 4. Ratio of the elastic scattering cross section to the Rutherford cross section for 65-MeV α particles on ^{89}Y, ^{94}Zr, and ^{96}Zr. The smooth curves are optical-model least-squares fits with the parameters given in Table I.

TABLE II. Potentials for $^{92}Zr+\alpha$ elastic scattering at 65 MeV. Parameters in parentheses were held constant during the searches with the extended data.

Potential	V_0 (MeV)	r_0 (F)	a (F)	W_0 (MeV)	r_0' (F)	a' (F)	σ_r (mb)	χ^2
K[a]	(34.36)	(1.554)	(0.662)	(18.92)	$r_0'=r_0$	$a'=a$	2019	780
L[a]	(75.00)	(1.426)	(0.661)	(39.34)	$r_0'=r_0$	$a'=a$	1996	572
M[a]	(200.0)	(1.277)	(0.665)	(97.68)	$r_0'=r_0$	$a'=a$	1988	596
N	70.44	1.434	0.660	36.18	$r_0'=r_0$	$a'=a$	1987	525
O	28.22	1.611	0.558	14.35	1.515	1.046	2331	609
P	79.66	1.397	0.699	22.04	1.547	0.595	1968	428
Q	212.6	1.267	0.663	98.45	1.261	0.673	1982	551
R	(247.0)	1.064	0.846	(17.00)	1.672	0.495	1970	1388

[a] Potential obtained from searches on data to 77°, Ref. 1. The χ^2 is obtained from comparison with the extended angular distributions.

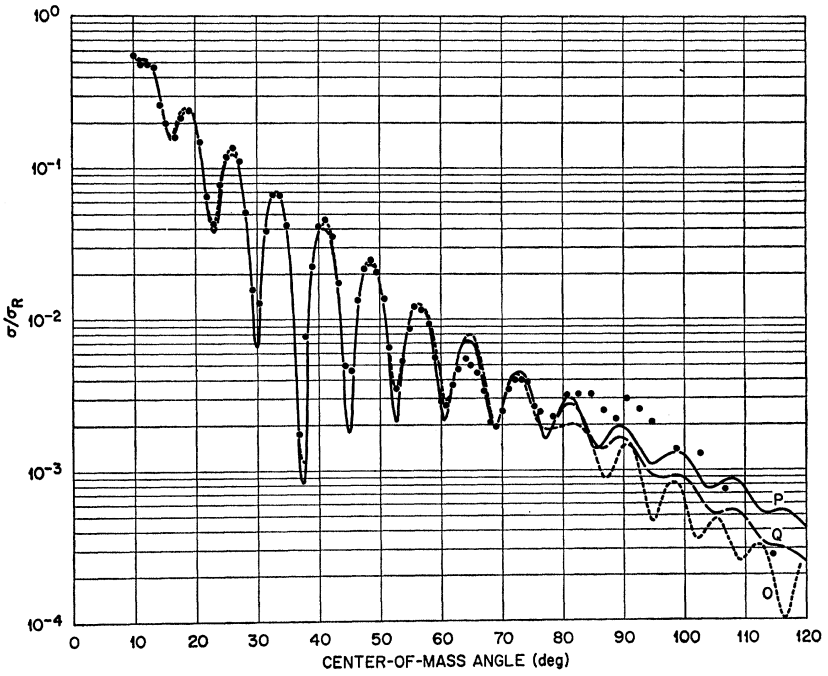

FIG. 5. Ratio of extended differential cross sections for elastic scattering to the Rutherford cross section of 65-MeV α particles from ^{92}Zr. The smooth curves are optical-model least-squares fits with the parameters given in Table II.

isotopes. This figure includes results from Ref. 1 and results of searches[4] on elastic scattering angular distributions for 64.3-MeV α particles on ^{58}Ni.[5] The smooth dependence of W_0, r_0, and a on V_0 results from the requirement that all the potentials be equivalent at large radii as proposed by Igo[6] and discussed in Refs. 1 and 7. Some systematic features appear in Fig. 6. For a given V_0, there tends to be a monotonic increase in W_0 and a monotonic decrease in r_0 with increasing atomic weight. The ^{89}Y, ^{90}Zr, and ^{58}Ni potentials are slightly less diffuse than the potentials for the other five nuclei.

Beyond 70°, the angular distributions predicted by the different potentials for a given nucleus are different. For example, the differential cross section at 110° (c.m.) for ^{92}Zr(α, α) predicted by the potential L (see Table II) is 3.44 times as large as for potential K. These potentials are among those obtained in Ref. 1 by fitting data from 10° to 77°. To capitalize on such differences, the experimental angular distributions were extended to about 115° (c.m.). The new data points, along with a representative sample of the earlier ones,[1] are shown in Fig. 5. Predictions of three previously reported potentials (K, L, and M) were compared with the extended data; the values of χ^2 are given in Table II. The shallow potential K which gave the best fit of the data up to 77° no longer gives the smallest χ^2; those for both L and M are smaller.

Several new searches were made for fits of the extended angular distributions. Potential N was the result of a search beginning with the four-parameter set L. Potentials O–R are six-parameter sets having independent geometry for the real and imaginary parts. Potentials O, P, and Q resulted from searches beginning with K, L, and M, respectively, and allowing all six parameters to vary. The resulting angular distributions are compared with the data in Fig. 5. The best-fit potential P is quite different from its predecessor L. Potentials O, P, and Q have different asymptotic behavior[1] since a, a', and W_0/V_0 are not the same for the three potentials. An attempt to find a potential with $V_0 \approx 200$ MeV having the same asymptotic behavior as potential P resulted in a large χ^2. When all the parameters were permitted to vary, the potential slowly migrated toward potential Q. Potential P therefore appears to give a local minimum.

Potential R was generated in an attempt to find an α-particle potential satisfying the criterion $V_\alpha(r) \approx V_{^3\mathrm{He}}(r) + V_n(r)$. Such a potential may be theoretically preferable for distorted-wave calculations of (α, ^{3}He) and (^{3}He, α) reactions.[8] For $V_{^3\mathrm{He}}(r)$ the best-fitting potential (potential A of Ref. 9) for the elastic scattering of 51.3-MeV ^{3}He from ^{92}Zr was used. For $V_n(r)$ a real Woods-Saxon potential with $V_0 = 50$ MeV, $r_0 = 1.2$ F, and $a = 0.7$ F was chosen. The α-particle parameters V_0 and W_0 were held fixed during the search, thus forcing the central region to obey the above criterion. The resulting potential (R) gave a very poor

[4] C. R. Bingham and M. L. Halbert, Phys. Rev. **169**, 933 (1968).
[5] P. Darriulat, G. Igo, H. G. Pugh, J. M. Meriwether, and S. Yamabe, Phys. Rev. **134**, B42 (1964).
[6] G. Igo, Phys. Rev. Letters **1**, 72 (1958); Phys. Rev. **115**, 1665 (1959).
[7] R. M. Drisko, G. R. Satchler, and R. H. Bassel, Phys. Letters **5**, 347 (1963).
[8] R. Stock, R. Bock, P. David, H. H. Duhm, and T. Tamura, Nucl. Phys. **A104**, 136 (1967).
[9] C. R. Bingham and M. L. Halbert, Phys. Rev. **158**, 1085 (1967).

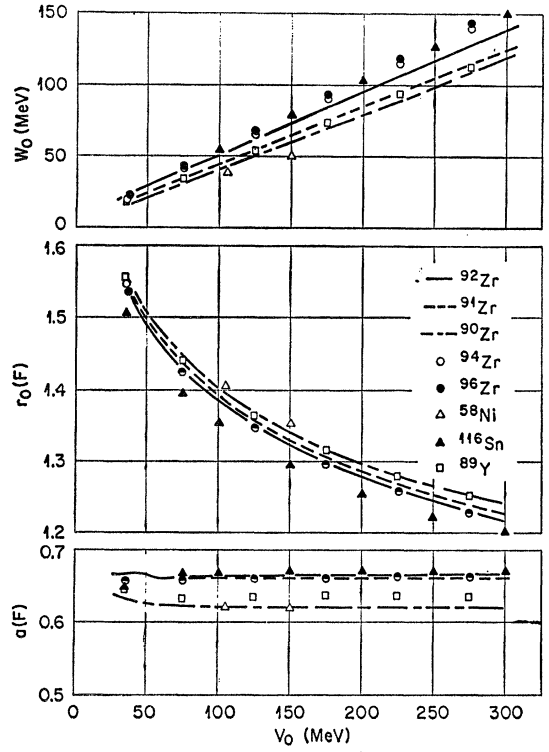

FIG. 6. Interdependence of optical-model parameters for α particles near 65 MeV. For each point V_0 was held fixed at the value shown while the other parameters were allowed to vary until a minimum in χ^2 was found.

fit at large angles. When V_0 and W_0 were permitted to vary also, the parameters migrated toward those of potential Q. When potential R was put into an (α, ^{3}He) calculation, the resulting angular distribution fit the data[1] very poorly. Radial cutoffs from 3 to 5 F affected the predictions drastically, but no cutoff improved the fit significantly. Apparently, if the interior of the potential is forced to correspond to that of ^{3}He+n, the surface region is affected to the extent that a good fit of (α, ^{3}He) cannot be obtained.

In previous analyses of elastic scattering angular distributions for ^{58}Ni at 43 MeV over a wide range of angles,[10] the six-parameter potential was found to be far superior to a four-parameter potential. While the best six-parameter potential (P) fits the present data better than the best four-parameter potential (N), the improvement is not large. The present angular distributions do not extend to as large angles as those of Ref. 10, but they do fall off much more rapidly and have as many maxima and minima.

IV. INELASTIC SCATTERING

Angular distributions were obtained for inelastic peaks at 0.92, 1.68, 2.12, and 3.04 MeV in ^{94}Zr; 1.9 MeV in ^{96}Zr; 1.29, 2.28, and 2.97 MeV in ^{116}Sn; and 0.93 and 2.35 MeV in ^{92}Zr. These are shown as points in Figs. 7–9. Figure 9 also contains representative points of the earlier ^{92}Zr(α, α') data.[1] For ^{89}Y, cross sections were obtained at 1° intervals from 35.8° to 38.8° (c.m.) for peaks at 1.51, 1.75, 2.22, 2.53, 2.84, 3.09, and 3.75 MeV. These four-point angular distributions are shown in Fig. 10.

Most of the calculations of the inelastic scattering angular distributions were made using the zero-range distorted-wave theory with collective-model form factors.[11] Only one-phonon transitions were considered. The deformation parameter β is the only adjustable parameter and is determined by normalization of the calculation to the experimental data.

Inelastic scattering has often been calculated with the assumption that only the real part of the optical potential is deformed in an inelastic scattering event. However, there has been ample evidence that both the real and imaginary parts are deformed,[12] and that the deformation of each part is about the same.[4] For the four-parameter optical potential, the angular distributions predicted by real and complex coupling are identical; for a given set of experimental data the deformation parameters obtained from complex coupling will be smaller by the factor $(1+W_0^2/V_0^2)^{1/2}$.

A. Scattering from ^{116}Sn, ^{94}Zr, ^{96}Zr, and ^{89}Y

The four-parameter potentials were used in the present analyses of scattering from ^{94}Zr, ^{96}Zr, ^{89}Y, and ^{116}Sn. Coulomb excitation was included in most of the Zr and Y calculations, although it produced only a small effect. It could not be included in the ^{116}Sn scattering calculations for lack of enough partial waves in the distorted-wave code JULIE,[13] but this probably made only a small difference in the predicted angular distributions.

The effect of the optical-model ambiguities was investigated. Any potential giving a good fit to the elastic scattering predicted the inelastic scattering well, and the deformation lengths $\beta_l R_0$ were the same ($R_0 = r_0 A^{1/3}$). The results reported here use potentials A, E, G, and I for scattering from ^{116}Sn, ^{89}Y, ^{94}Zr, and ^{96}Zr, respectively.

The distorted-wave predictions are compared with the experimental angular distributions for ^{94}Zr, ^{96}Zr, and ^{116}Sn in Figs. 7 and 8. The corresponding deformation parameters are given in Table III. To facilitate comparison with other experiments, values of β_l and $\beta_l R_0$ are given for both real and complex coupling. The large inelastic peak in ^{96}Zr contained both the 2^+ and 3^- states. The angular distribution was fitted with a linear combination of 2^+ and 3^- JULIE predictions.

[10] H. W. Broek, J. L. Yntema, B. Buck, and G. R. Satchler, Nucl. Phys. **64**, 259 (1965).

[11] R. H. Bassel, G. R. Satchler, R. M. Drisko, and E. Rost, Phys. Rev. **128**, 2693 (1962).

[12] E. R. Flynn and R. H. Bassel, Phys. Rev. Letters **15**, 168 (1965); see also Refs. 9 and 10.

[13] Written by R. M. Drisko.

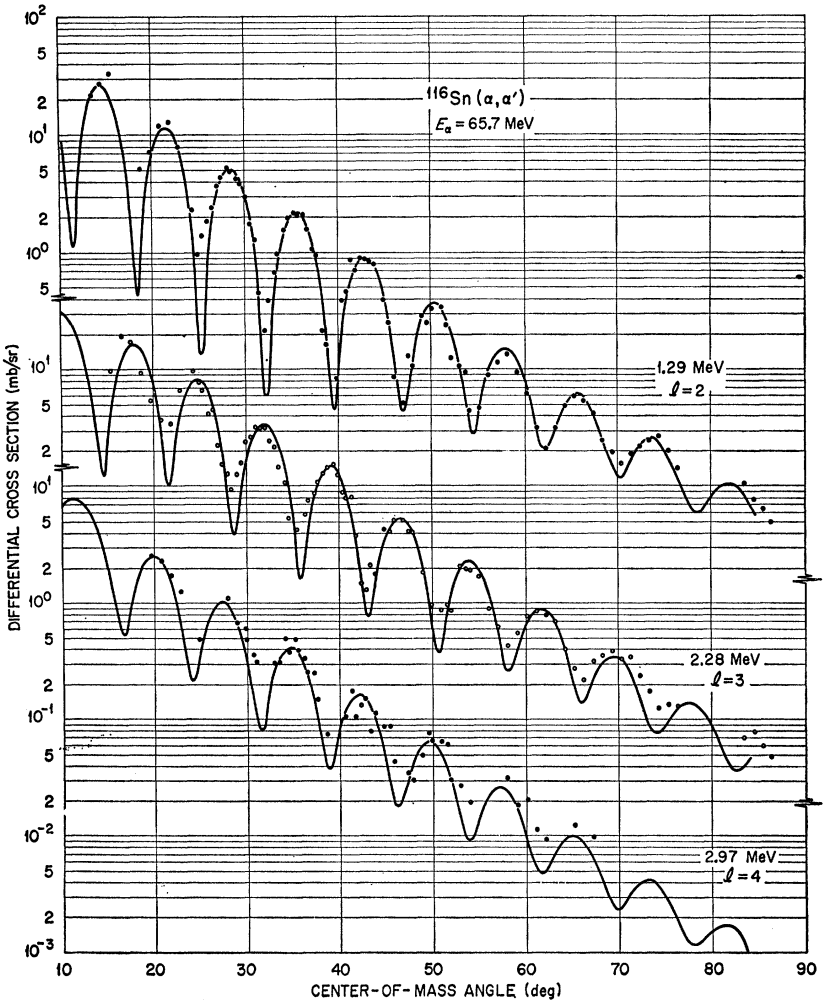

FIG. 7. Angular distributions for ^{116}Sn(α, α′) at 65.7 MeV in comparison with distorted-wave calculations.

TABLE III. Results of inelastic scattering from ^{94}Zr, ^{96}Zr, and ^{116}Sn.

Target	E^* (MeV)	l	Present experiment: Real interaction β_l	Real interaction $\beta_l R_0$	Complex interaction β_l	Complex interaction $\beta_l R_0$	Other experiments β_l	Other experiments $\beta_l R_0$
^{116}Sn	1.29	2	0.120	0.881	0.103	0.759	0.128,[a] 0.13[b]	0.696,[a] 0.93[b]
^{116}Sn	2.28	3	0.136	0.998	0.117	0.860	0.15[b]	1.068[b]
^{116}Sn	2.97	4	0.064	0.470	0.055	0.405		
^{94}Zr	0.92	2	0.106	0.745	0.092	0.643	0.12[c]	0.66[c]
^{94}Zr	1.68	2	0.058	0.407	0.050	0.351	0.075[c]	0.41[c]
^{94}Zr	2.12	3	0.178	1.25	0.154	1.08	0.19[c]	1.04[c]
^{96}Zr	1.9[d]	2	0.089	0.625	0.076	0.536	0.088,[e] 0.13[f]	0.464,[e] 0.71[f]
		3	0.200	1.40	0.172	1.20	0.27[f]	1.48[f]

[a] Coulomb excitation, Ref. 17. The results are corrected for a rounded charge distribution; see Ref. 19.

[b] Inelastic scattering of 40-MeV α particles, real interaction, Ref. 14.

[c] Inelastic scattering of 19.4-MeV protons, complex interaction, Ref. 15.

[d] Doublet containing 2^+ and 3^- states. According to Ref. 16, the 2^+ state is at 1.72 MeV and the 3^- is at 1.86 MeV.

[e] β_2 calculated from the Coulomb excitation $B(E2)$ of Ref. 18 according to prescription of Ref. 17. The results are corrected for a rounded charge distribution; see Ref. 19.

[f] Inelastic scattering of 19.4-MeV protons, complex interaction, Ref. 16.

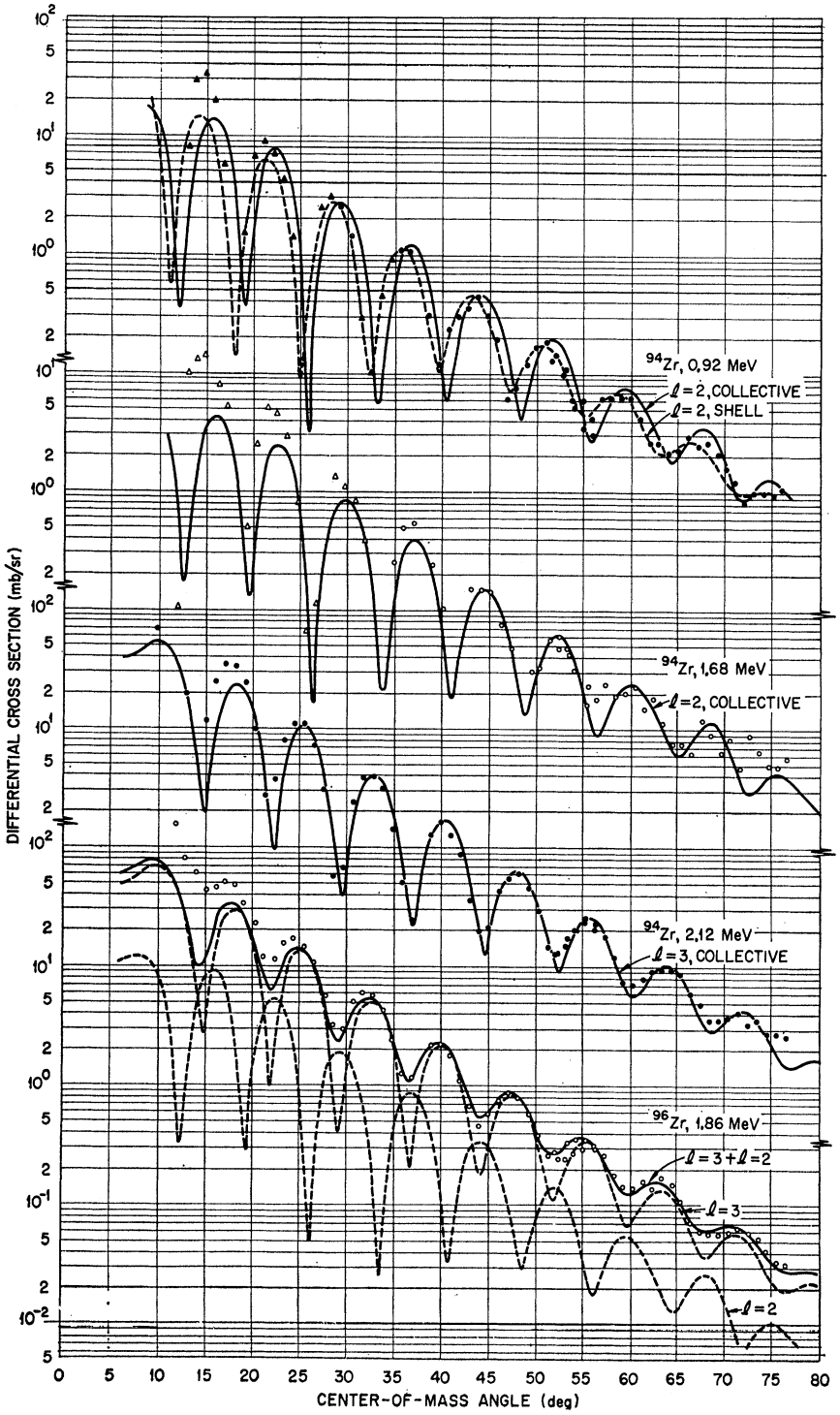

FIG. 8. Angular distributions for $^{94}Zr(\alpha, \alpha')$ and $^{96}Zr(\alpha, \alpha')$ at 65 MeV in comparison with distorted-wave calculations. The ^{96}Zr peak contains a 2^+ and a 3^- state. The data are fitted with the sum of the 2^+ and 3^- curves shown.

Each component along with the sum is shown in Fig. 8. Since the 3^- contribution is dominant, β_3 is determined better than β_2. A peak was found at 3.04 MeV in ^{94}Zr. It was too weak to analyze properly, but it showed qualitative resemblance to a 4^+ calculation.

The deformation lengths $\beta_l R_0$ agree well with other scattering experiments[14–16] except for the ^{96}Zr results.

[14] N. Baron, R. F. Leonard, John L. Need, W. M. Stewart, and V. A. Madsen, Phys. Rev. **146**, 861 (1966).

[15] M. M. Stautberg and J. J. Kraushaar, Phys. Rev. **151**, 969 (1966).

[16] M. M. Stautberg, R. R. Johnson, J. J. Kraushaar, and B. W. Ridley, Nucl. Phys. **A104**, 67 (1967).

The Coulomb excitation results[17,18] do not agree as well, but if corrections are made for a rounded charge distribution,[19] the agreement improves.

The four-point angular distributions for $^{89}Y(\alpha, \alpha')$ are shown in Fig. 10. The angular distributions for the 1.51- and 1.75-MeV levels are out of phase with the elastic scattering angular distributions, while those for the levels at 2.22, 2.53, and 3.75 are definitely in phase. This is consistent with $l=2$ and $l=3$ assignments made in other scattering experiments[20–22] for these two groups of states, respectively. The angular distributions for groups at 2.84 and 3.09 MeV also appear to be in phase with the elastic peak but with much less variation of cross section than for the three $l=3$ states listed above, making it difficult to draw any conclusions about them.

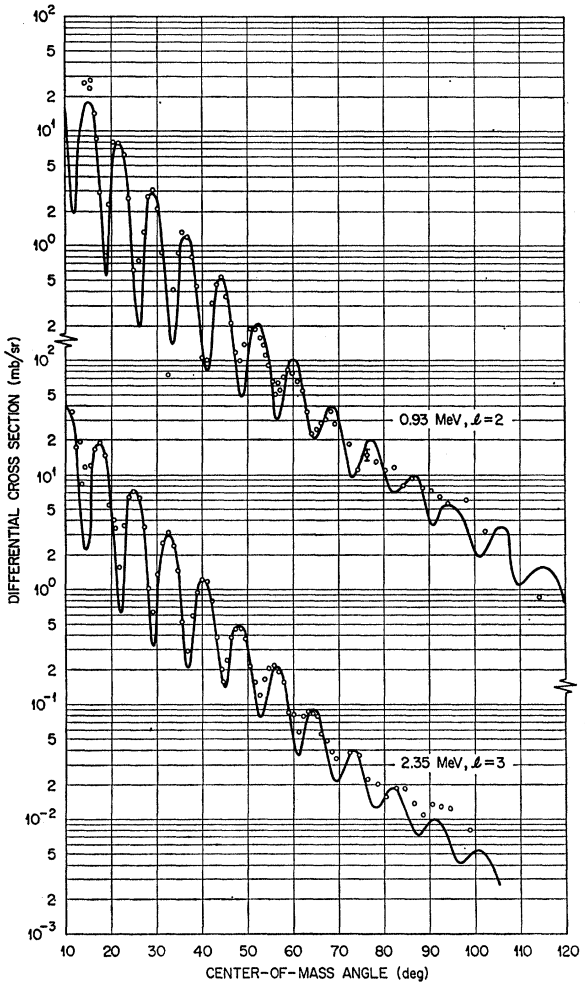

FIG. 9. Extended angular distributions for $^{92}Zr(\alpha, \alpha')$ at 65 MeV in comparison with distorted-wave calculations.

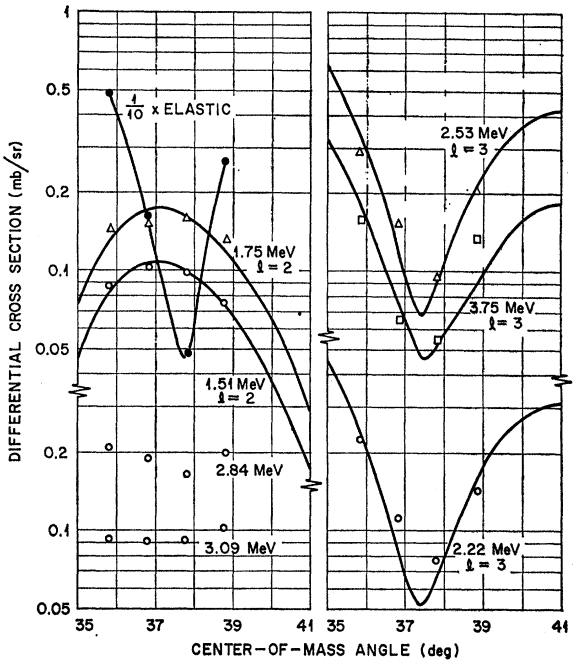

FIG. 10. Angular distributions for $^{89}Y(\alpha, \alpha')$ at 65 MeV in comparison with distorted-wave calculations. To facilitate comparison with the Blair phase rule, the elastic scattering angular distribution is also shown.

Although the angular distributions are quite limited, it is of interest to obtain estimates of the deformation lengths. Distorted-wave calculations were made for four of the inelastic groups. Spin assignments from other experiments, as discussed in Ref. 20, were used. The predictions are shown in Fig. 10 in comparison with the data. The deformation parameters are compared with those of the other experiments in Table IV. The errors on the deformation parameters obtained here should be about ±15% for the odd-parity states and ±25% for the even-parity states, if we judge by the agreement of the experimental and theoretical angular distributions near 37° in the Zr isotopes.[1] The present results agree fairly well with the (p, p') and (^{3}He, ^{3}He′) results[20,21] but disagree with (α, α') results[22] at 42 MeV. Since the 42-MeV (α, α') results were obtained from the adiabatic approximation of Austern and Blair,[23] while the distorted-wave theory was used in the other three experiments, it is not clear that the βR are defined in the same way.

It is of interest to compare the results with a model which weakly couples the odd nucleon to the collective states of the even-even core. For ^{89}Y, the odd nucleon is in a $p_{1/2}$ orbit, so an $l=2$ transition in the ^{88}Sr core

[17] P. H. Stelson and F. K. McGowan, Phys. Rev. **110**, 489 (1958).
[18] Yu. P. Gangrskii and I. Kh. Lemberg, Yadern. Fiz. **1**, 1025 (1965) [English transl.: Soviet J. Nucl. Phys. **1**, 731 (1965)].
[19] L. W. Owen and G. R. Satchler, Nucl. Phys. **51**, 155 (1964).
[20] M. M. Stautberg, J. J. Kraushaar, and B. W. Ridley, Phys. Rev. **157**, 977 (1967).
[21] E. F. Gibson, J. J. Kraushaar, B. W. Ridley, M. E. Rickey, and R. H. Bassel, Phys. Rev. **155**, 1208 (1967).
[22] J. Alster, D. C. Shreve, and R. J. Peterson, Phys. Rev. **144**, 999 (1966).
[23] N. Austern and J. S. Blair, Ann. Phys. (N.Y.) **33**, 15 (1965).

TABLE IV. Results of inelastic scattering from ^{89}Y.

			(α, α')[a]				(p, p')[b,c]		$(^3\text{He}, ^3\text{He}')$[c,d]		(α, α')[e]
			Real int.		Complex int.						
E^* (MeV)	l	J_f	β_l	$\beta_l R_0$ (F)	β_l	$\beta_l R_0$ (F)	β_l	$\beta_l R_0'$ (F)	β_l	$\beta_l R_0'$ (F)	$\beta_l R_0$ (F)
1.51	2	$\frac{3}{2}^-$	0.047	0.33	0.042	0.29	0.065	0.36	0.045	0.32	0.14
1.75	2	$\frac{5}{2}^-$	0.049	0.34	0.044	0.31	0.060	0.34	0.046	0.33	0.20
2.22	3	$(\frac{5}{2}^+)$	0.109	0.76	0.097	0.67	0.11	0.60	0.069	0.49	0.26
2.53	3	$\frac{7}{2}^+$	0.109	0.76	0.097	0.67	0.11	0.60	0.074	0.53	0.33
3.75	(3)	$\frac{5}{2}^+$	0.086	0.60	0.077	0.53			0.051	0.37	0.19

[a] This experiment.
[b] Reference 20.
[c] Complex interaction used.
[d] Reference 21.
[e] Reference 22. Adiabatic approximation of Austern and Blair (see Ref. 23) used.

would populate $\frac{3}{2}^-$ and $\frac{5}{2}^-$ states while an $l=3$ transition would populate $\frac{5}{2}^+$ and $\frac{7}{2}^+$ states. Hence, one could form the 1.51- and 1.75-MeV states with spin assignments[20] of $\frac{3}{2}^-$ and $\frac{5}{2}^-$ by coupling the $p_{1/2}$ odd proton to the first 2^+ level at 1.84 MeV in ^{88}Sr, and the $\frac{5}{2}^+$ and $\frac{7}{2}^+$ levels at 2.22 and 2.53 MeV by coupling the $p_{1/2}$ proton to the 3^- level at 2.74 MeV in ^{88}Sr. According to the weak-coupling theory, the deformation parameters for the 1.51- and 1.75-MeV levels in ^{89}Y, and the 1.84-MeV level in ^{88}Sr should be equal. Likewise, the deformation parameters for the 2.22- and 2.53-MeV levels in ^{89}Y and the 2.74-MeV level in ^{88}Sr should be equal. The ratios of the experimental deformation parameters for the 1.51- and 1.75-MeV states and for the 2.22- and 2.53-MeV states are very close to unity, in agreement with the weak-coupling theory. However, the deformation length for each of the $l=2$ transitions in ^{89}Y differs from the deformation length obtained from (p, p')[20] for the 2^+ level of ^{88}Sr by a factor of $\sim 0.30/0.65=0.46$, or the cross sections in ^{89}Y are lower by a factor of about 4. The deformation length for each of the $l=3$ transitions in ^{89}Y differs from that[20] for the 3^- state of ^{88}Sr by a factor of $0.67/0.75=0.89$. It appears that the weak-coupling theory makes reasonably good predictions for the strengths of the $l=3$ transitions but poor ones for the $l=2$ transitions.

The collective-model distorted-wave prediction for the 2^+ state in ^{94}Zr is slightly shifted with respect to the data. A calculation treating the transition as a single-particle excitation[24] was made. The α-particle nucleon interaction was assumed to be a Gaussian with a range of 2.0 F. The strength of the interaction was adjusted to normalize the calculation to the data. The ground-state and 0.92-MeV level were assumed to be $(d_{5/2})_0^{-2}$ and $(d_{5/2})_2^{-2}$ configurations. The distorted-wave form factors were computed with the code ATHENA[25] under the following conditions: The radial wave functions were those for a neutron in a Woods-Saxon potential with $r_0=1.2$ F, and $a=0.7$ F, and with a spin-orbit term equal to 25 times the Thomas term. The depth of the potential was adjusted to give the binding energy of the neutron in the ground state of ^{91}Zr. The wave functions for an equivalent nonlocal potential, with a range of 0.85 F, were obtained in the local-energy approximation.[26] The form factors were then used in the distorted-wave code JULIE to obtain the angular distribution.

The result is the dashed curve in Fig. 7 and agrees with the data somewhat better than the collective-model prediction. The strength of the interaction required was 52.8 MeV, which does not agree with the value of 73.8 MeV from a similar calculation for the 2^+ state of ^{92}Zr at 0.93 MeV.[1] Although the angular distribution for the peak at 3.04 MeV was not definitive, its interpretation as the $(d_{5/2})_4^{-2}$ state yields an interaction strength of 47.8 MeV, in good agreement with the result above.

B. Extended Data for ^{92}Zr

The inelastic scattering angular distributions to the 2^+ and 3^- states of ^{92}Zr at 0.93 and 2.35 MeV were recalculated with the new potentials, including Coulomb excitation. The predictions shown in Fig. 9 were obtained from the best-fit potential (P) with complex coupling. A real interaction seemed to fit the data as well as a complex interaction. The deformation parameters agree with those previously reported.[1]

ACKNOWLEDGMENTS

The authors wish to thank D. O. Galde and B. D. Belt for their aid in analyzing the data, the ORIC operations staff for their cooperation during the runs, and R. H. Bassel for helpful comments.

[24] G. R. Satchler, Nucl. Phys. **77**, 481 (1966).
[25] Written by M. B. Johnson and L. W. Owen.
[26] F. G. Perey and A. M. Saruis, Nucl. Phys. **70**, 225 (1965).